Electronic Supplementary Material (ESI) for Lab on a Chip.

Supplementary Information for:

Low-cost and rapid prototyping of electrochemical microfluidic biosensors using consumer-grade off-the-shelf tools and materials

Mohd Afiq Mohd Asri [1], Wing Cheung Mak [2, 3], Siti Azizah Norazman [1], and Anis Nurashikin Nordin [1]*

[1] Department of Electrical and Computer Engineering, Kulliyyah of Engineering, International Islamic University Malaysia, 53100 Gombak, Selangor, Malaysia

[2] Biosensors and Bioelectronics Centre, Department of Physics, Chemistry and Biology (IFM), Linköping University, 58183, Linköping, Sweden

[3] Department of Biomedical Engineering, The Chinese University of Hong Kong, Shatin, Hong Kong

*Corresponding author: anisnn@iium.edu.my

Contents

Optimizing Silhouette Cameo Parameters

Prior to optimizing cutting and plotting parameters, several combinations of materials were identified as critical to the project. These combinations of materials were then tested for a combination of Silhouette Cameo® parameters: blade depth (0.1 – 1 mm), speed (1-10), downward force (1-33), and number of passes. Testing of cuttability is performed using Silhouette's 'test cut' function which cuts a small 2 × 2 mm square with a smaller triangle inside. Following early optimization, the setting used for each type of cut/sketch is as listed in Table S1 and used consistently throughout the project.

Table S1. Summary of Silhouette Cameo® settings for specific combination of materials.

	Settings for:	**Mode of action**	**Blade Depth**	**Speed**	**Force**	**Passes**	**Overcut**
1	Vinyl sticker on plain PET (through vinyl only)	Cut	1	1	8	1	Yes
2	Gold leaf and ultrathin tape on PET (through tape only)	Cut	1	1	25	1	Yes
3	Plain/resin-coated PET (edge cut), through-cut	Cut	6	1	30	2	Yes
4	Plain/resin-coated PET (small holes), through-cut	Cut	6	1	30	3	Yes
5	HeatNBond-PET-HeatNBond sandwich, through-cut	Cut	7	1	30	3	Yes
6	G9900 pressure sensitive adhesive, through-cut	Cut	8	1	30	3	Yes
7	Circuit Scribe silver pen, drawing	Sketch	-	1	16	2	-

Resolution limits for combinations of materials being cut by the Silhouette Cameo was explored to define design and fabrication process specifications. Designing micro-structured features smaller than these limits will likely result in fabrication failure, either structural or electrical. These limits are summarized in Table S2.

Table S2. Resolution limits for different combinations of materials.

	Process	**Minimum line width (µm)**	**Minimum diameter (µm)**	**Minimum gap width (µm)**	**Height (µm)[1]**
1	Vinyl stencil on pristine PET film (general purpose stencil)	250	500	250	76–153
2	CircuitScribe silver interconnects on resin-coated PET film	385	685	300	~10
4	Cut gold leaf mounted using Teraoka 7070W ultrathin double-sided tape on pristine PET, followed by vinyl lift-off	400	3000	~45	~11
5	Cut gold leaf mounted using Teraoka 7070W ultrathin double-sided tape on pristine PET, without vinyl lift-off	250	1200	~45	~11
6	Microchannels in HNB-PET-HNB sandwich	300	1200	1000	~300
7	Square inlets/outlets on pristine PET film	-	800	-	-

[1] Height is determined through several assumptions on material thicknesses: vinyl stickers are typically sold as 3 mil (76 µm), 4 mil (101.5 µm), 5 mil (127 µm) or 6 mil (153 µm). Other materials are based on thicknesses provided by manufacturers: gold leaf is 120 nm, Teraoka ultrathin double-sided tape is 10 µm, HeatNBond iron-on adhesive is 100 µm, PET film is 100 µm.

Table S3. Selected physical properties of polyethylene terephthalate (PET) related to microfluidics applications [1–4].

Property	Value (unit)	Notes
Molecular weight (of repeating unit)	192 (g mol^{-1})	
Density	1.41 (g cm^{-3})	
Glass transition temperature	69 – 115 (°C)	Useful information for materials processing
Melting temperature	265 (°C)	
Tensile strength	55 – 75 (MPa)	
Young's modulus	2800 – 3100 (MPa)	
Refractive index	1.575	Necessary information for microfluidic designs with optical integration
Thermal conductivity	0.15 – 0.24 (W/m K)	Necessary information for microfluidic designs with heat transfer applications
Heat capacity	1.0 (kJ/kg K)	
Critical surface tension	0.0043 (N/m)	Low surface energy, presents challenges for adhesion
Oxygen permeability / diffusion coefficient	3.3×10^{-13} m^2/s	Very low gas permeability
Carbon dioxide permeability / diffusion coefficient	6.8×10^{-14} m^2/s	
Solubility in water	-	Practically insoluble

Bill of Materials and Cost Analysis

The primary goal of this project is to develop a low-volume device manufacturing process (i.e. prototyping) that is low cost. To evaluate the cost-efficiency of the fabrication process, the bill of materials in the finalized and optimized process is assessed in Table S3 to provide an insight on the upfront cost for setting up the system. Additionally, the estimated cost breakdown of one unit of device manufactured using this process is evaluated in Table S4. The assumptions used when estimating the unit device cost is included at the end of the table.

Table S4. Bill of materials and breakdown of upfront cost for setting up system.

	Availability	**Cost (MYR)[2]**	**Cost (USD)[3]**
Equipment[1]			
Silhouette Cameo® 3 plotter cutter	Silhouette online store	1280	320
Silhouette Cameo® 3 pen holder	Silhouette online store	40	10
Ta-Peer 101 laminator	Online store / off-the-shelf	160	40
TOTAL EQUIPMENT		***1480***	**370**
Consumables, minimum order quantity			
ProMaster O.H.P Transparency film, A4 size, 100 microns, 100 sheets	Online store / off-the-shelf	45	11.25
Inkjet transparency film, resin-coated PET, A4 size, 10 sheets	Online store / off-the-shelf	32	8.00
HeatNBond Ultrahold Iron-On Adhesive, 43 x 93 cm sheet	Online store / off-the-shelf	38	9.50
Vinyl sticker, 50 cm × 100 cm roll	Online store / off-the-shelf	10	2.50
Teraoka 7070W ultrathin double-sided tape, 3 cm × 50 m	Online store (Monotaro)	260	65.00
Edible gold leaf 23 karat, 25 mm x 25 mm, 100 sheets	Online store	80	20.00
Circuit Scribe silver conductive ink pen	Online store / off-the-shelf	120	30.00
Isopropyl alcohol, 99%, 500 mL	Online store / off-the-shelf	15	3.75
TOTAL CONSUMABLES		***600***	**150**
TOTAL UPFRONT COST (RM)		**2080**	**520**

[1] Excludes items used in this work that are assumed common to typical labs: micropipettes, pipette tips, deionized water, tweezers, scissors, box cutters, weighing balances, etc.

[2] Costs are accurate at time of purchase, inclusive of shipping costs. Costs listed are due purchases from Malaysia and may be different if purchased from a different country or region.

[3] Conversion rate at the time of writing is 1.00 MYR = 4.00 USD.

Table S5. Cost estimate per unit for an electrochemical microfluidic biosensor in this work.

Unit consumable[1]	**Cost per unit consumable (MYR)**[2]	**Sensors made per unit consumable**[3]	**Contribution to sensor cost (MYR)**
PET transparency film, 1 pc A4 sheet	RM0.45	144	RM0.003
Inkjet PET transparency film, 1 pc A4 sheet	RM2.80	144	RM0.019
Teraoka 7070W ultrathin double-sided tape, 3 cm x 3 cm	RM0.16	1	RM0.16
CircuitScribe silver conductive ink pen (~0.05 mL per A4 sheet)	RM0.60	144	RM0.004
Vinyl sticker, 1 pc A4 sheet (21 cm x 29.7 cm)	RM1.25	144	RM0.009
HeatNBond Ultrahold Iron-On adhesive, 1 pc A4 sheet (21 cm x 29.7 cm)	RM5.93	72	RM0.082
23K edible gold leaf, 25 mm x 25 mm, 1 pc	RM0.80	4	RM0.20
		ESTIMATED COST PER UNIT DEVICE[4]	RM0.48 (USD 0.12)[5]

[1] Cost estimated based on usage for one batch (typically A4 sheet sized).

[2] Cost of minimum order quantity divided by unit used in one batch of manufacturing.

[3] Estimated for sensors of size 10 mm × 20 mm. Devices were fabricated in clusters of 4 (to maximize use of gold leaf), and an A4 sheet of substrates conservatively may fit a 6 × 6 cluster array. (Theoretically a 10 × 7 cluster array is possible on an A4 sheet, however in practice a larger spacing between clusters are necessary to perform fabrication comfortably for manual processes such as removing vinyl negatives and applying gold leaf).

[4] Rounded up to the nearest cent (two decimals).

[5] Conversion rate at the time of writing is 1.00 MYR = 4.00 USD.

The cost estimate for biosensor devices of size 10 × 20 mm within a 6 × 6 cluster array (see definitions in Table S4 Note 3) is USD 0.12, excluding costs of chemical and biological reagents. When building larger sized devices, this cost may be multiplied by a factor of 2 or 4, or in cases where a device requires two gold leaf pieces, by a factor of 8. At maximum cost, an electrochemical microfluidic device fabricated using this method would cost USD 0.96 per unit.

Table S6. Estimated time taken for the steps involved in the fabrication process.

Process	**Time taken**
CAD design [1]	15 – 90 minutes
Device Fabrication	45 minutes
Gold leaf microelectrodes layer fabrication (N=4)	*20 minutes*
Ag reference electrode layer fabrication (N=4)	*10 minutes*
Fluidic circuit fabrication (N=4)	*10 minutes*
Device assembly (N=4)	*5 minutes*
PROCESS TIME, TOTAL [1]	**1 – 2 ¼ hours**

[1] CAD design time depends on user experience on using a CAD software. Here it is assumed that a user is fairly used to a CAD design suite and spends between 60 – 90 minutes for a new design, and 15 minutes for a design revision during an iteration cycle.

[2] The minimum process time of 1 hour assumes a quick iterative CAD design revision (15 minutes) and a fabrication-only process (45 minutes). The maximum process time of 2.25 hours assumes a new CAD design from scratch (90 minutes), and a full fabrication (45 minutes) process.

CAD Design Guidelines

Three rules apply for CAD design associated to the fabrication process, particularly for the design of vinyl stencil masks:

1. The spacing between gold leaf design outline and the vinyl stencil cut lines should be a minimum of 500 µm.
2. The opening on a vinyl stencil at any point should be more than 2 mm in width. Narrower opening will result in the ultrathin tape not mounted properly onto the PET substrate.
3. Avoid removing all of vinyl stencil with a single peel. Section cuts should be introduced into the design to reduce stress applied to the gold leaf due to stencil peeling.

These CAD design guidelines are illustrated in Figure S1.

Additionally, it is also important to note the size of gold electrode gaps as part of the design. Virtually, this feature is designed as a line of 'zero' thickness, however surface profilometry analysis suggests that this gap is ~45 µm, with approximately 9 µm variation. Geometrically, this translates to the gold leaf reducing ~22 µm in size for each side of a cut line. For example, a wire of linewidth 500 µm in the design software will be realized as approximately 455 µm wire, and a circular electrode of diameter 2 mm will be reduced to approximately 1.98 mm.

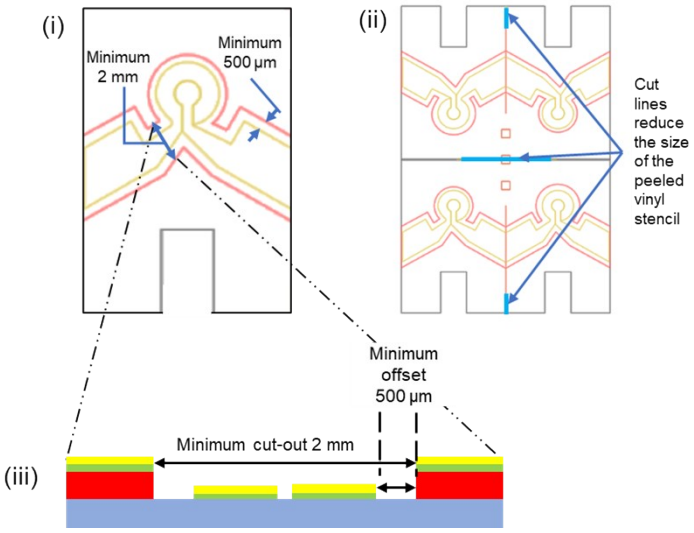

Figure S1. (a) Illustration showing examples of design rules regarding minimum distance between vinyl and gold leaf cut lines (500 µm), and minimum stencil opening of 2 mm. (b) Illustration showing cut lines (light blue) added to reduce the size of peeled vinyl stencils. The stencil will be peeled along red and light blue lines. (c) Cross sectional illustration of the design rules in (a).

For gold leaf designs, the design should be placed at a minimum of 30 mm below the (0, 0) position in Silhouette Studio software. This is to ensure that the design is not physically under the tool carrier and x-axis rail of the Silhouette Cameo®, which will obstruct the process of peeling vinyl mask and applying gold leaf onto the substrate.

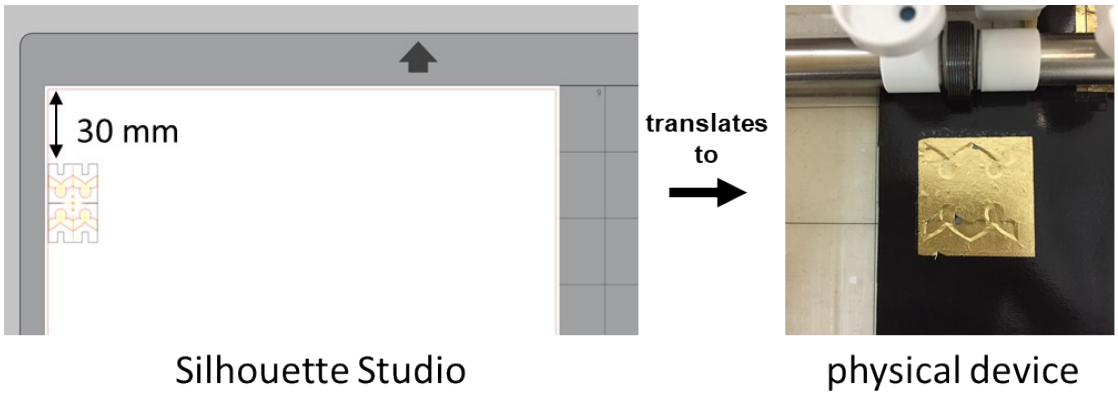

Figure S2. Positioning of the gold leaf electrode designs in Silhouette Studio. A placement of 30 mm below the origin point avoids the obstruction of access to the device by the tool carrier and x-axis rail.

For the Circuit Scribe CAD designs, inward offsets of 300 µm are used for filling in the geometry of the electrode, as exemplified in Figure S3.

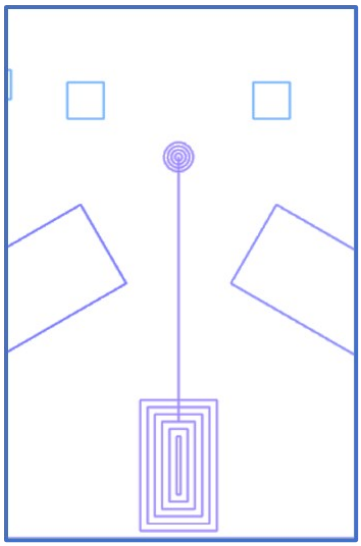

Figure S3. Offset filling of Circuit Scribe-drawn silver electrodes (shown in purple) in Silhouette Studio.

Microfluidic characterization

Burst pressure test

Burst pressure of the PET-HNB-PET-HNB-PET fluid channels is estimated by running dye through a single microchannel device at increasing volumetric flow rate. A single microchannel device (L=30 mm, w=300 µm, h=300 µm) is fabricated and the inlets and outlets of the device is adhered to a custom 3D-printed PLA connector using a pressure sensitive adhesive gasket (G9900; Dexerials, Tokyo, Japan; samples used were courtesy of Hitachi High-Technologies (Singapore) Pte Ltd.) connected to a syringe pump via Tygon tubing (#2375, I.D × O.D 1.6 × 3.2 mm) as shown in Figure S7. Increasing flow rates are applied into the device in 0.5 mL/min increments until dye leakage is seen through the laminated layers. Burst pressure is then determined through the following equation (adapted from Akbari et al [5] and solved for rectangular cross-section microchannels):

$$\Delta P = \left[16\pi^2 \mu I_p^* \frac{L}{A^2}\right] Q$$

$$I_p^* = \frac{1 + \left(\frac{a}{b}\right)^2}{12\left(\frac{a}{b}\right)}$$

Where ΔP is the pressure drop (N m^{-2}), Q is the flow rate (m^3 s^{-1}), μ is viscosity (water = 8.9 × 10^{-4} N m^{-2} s at 25 °C), I_p* is the specific polar moment of inertia (dimensionless), L is the characteristic length of the fully developed laminar flow (m), A is the cross-sectional area of the microchannel, a and b are the width and height the microchannel (m).

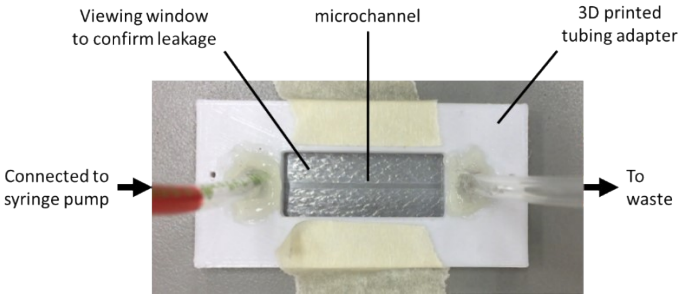

Figure S4. Experimental setup for burst pressure test.

A triplicate measurement yielded a burst flow rate of **3.0 ± 0.5 mL/min**. Using this data and the above equation, the estimated pressure drop across the inlet and outlet is calculated:

Q	5 × 10^{-8} ± 8.3 × 10^{-9}	m^3 s^{-1}
μ	0.00089	N m^{-2} s
I_p*	0.166667	
L	0.02	m
A	0.00000009	m^2

Which yielded **ΔP = 2.892 ± 0.482 kPa**. (1 Pa = 1 N m^{-2})

Microfluidic laminar flow test

Laminarity of the device is evaluated using a Y-junction merging microchannel device (two inlets, one outlet) with both top and bottom walls consist of plain PET sheets. Red and blue dyes are pumped into the inlets at 6 µL min^{-1} using electronic syringe pumps and the microchannel is imaged and recorded using phone camera (iPhone 6, Apple Inc.). The color profile across the width of the merged flow is then analyzed using ImageJ RGB profiler to determine laminar separation [6,7]. It can be observed in Figure S8 that the two dyes do not mix within the merging channel, a characteristic of laminar flow.

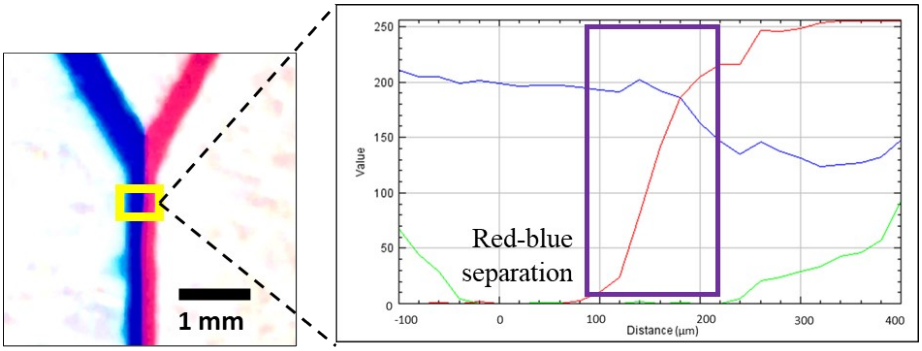

Figure S5. Image of dye flow merging in microchannel with pristine PET as its surface. RGB color profilogram across the width of the microchannel, showing that there is no mixing between the separated dye flow due to its laminar properties.

We then proceeded to estimate the Reynolds' number of the devices. Microfluidic devices consisting of a microchannel (L = 20 mm, w = 300 µm) with single inlet and outlet is fabricated using plain PET as bottom layer, resin-coated PET as top layer, and HeatNBond as adhesive. 10 µL of red dye is carefully placed on the inlet of the device using micropipette, without applying any air pressure. Dye is driven into the microchannel through capillary action and the flow is video recorded. From the video footage, the velocity of the flow can be determined, and the device's Reynolds number is then calculated using the equation:

$$Re = \frac{L}{v}u$$

Where v is kinematic viscosity of water 1.0 × 10^{-6} m^2 s^{-1} at 25 °C, L is characteristic length of microchannel (L = 10 mm), and u is the fluid front velocity. The apparent fluid flow velocity and the corresponding Reynolds' number are recorded in Table S7.

Table S7. Apparent fluid front velocity measured from video analysis of passive dye flow in microchannels, and corresponding Reynolds number.

Run	Apparent fluid front velocity (m/s)	Reynolds number
1	0.0104	3.4989
2	0.0082	2.7588
3	0.0065	2.1868
Average	**0.00837 ± 0.00160**	**2.8148 ± 0.5371**

An experimental Reynolds number of 2.815 shows that the flow in the HeatNBond-based microfluidic device is laminar, well below the laminar–turbulent transitional region (Re > 2000). This allows us to proceed with assumptions applicable to standard microfluidic principles when designing microdevices.

Comparison to commercial systems

This section contains supplementary information for section "Performing electrochemistry using fabricated sensors".

Table S8. Table comparing important parameters from the sensor in this work and DropSens SPGE. Measurements were performed in triplicates. P-values with asterisks suggest that the differences in parameter values for the two sensors are statistically significant.

	Half-cell potential, $E_{1/2}$	Peak separation, ΔE_p
This work	159.41 ± 5.45 mV	91.31 ± 5.69 mV
DropSens SPGE	165.09 ± 2.69 mV	68.89 ± 3.83 mV
Difference (p-value, Welch's two-tailed test)	5.68 mV (p = 0.251)	22.42 mV (p = 0.012*)
	Oxidation peak current density, J_{ox}	Reduction peak current density, J_{red}
This work	5.163 ± 0.452 µA mm^{-1} (RSD = 8.75%)	-5.495 ± 0.355 µA mm^{-1} (RSD = 6.46%)
DropSens SPGE	7.786 ± 0.028 µA mm^{-1} (RSD = 0.36%)	-7.913 ± 0.040 µA mm^{-1} (RSD = 0.51%)
Difference (p-value, Welch's two-tailed test)	2.623 µA mm^{-1} (p = 0.015*)	2.418 mm^{-1} (p = 0.011*)
	$J_{gold\ leaf}$ / $J_{DropSens}$, oxidation peak	0.663
	$J_{gold\ leaf}$ / $J_{DropSens}$, reduction peak	0.694

Characterisation of baseline parameters for electrochemistry

This section contains supplementary information for section "Performing electrochemistry using fabricated sensors".

Table S9. Measured peak separation for scan rates from each replicate (n=3) from ferrocyanide redox cycling on the electrochemical microfluidic biosensor device.

Scan rate (mV/s)	Peak separation, E_{p-p} (mV)
20	95.21
20	83.01
20	100.1
40	90.33
40	83.01
40	90.33
60	90.33
60	80.57
60	92.78
80	92.78
80	87.89
80	97.66
100	92.78
100	92.77
100	100.1
Average E_{p-p}	**91.31 ± 5.69 mV**

Determination of hydrogen peroxide peak by cyclic voltammetry

To determine the appropriate potential window to measure gold-catalyzed hydrogen peroxide reduction, cyclic voltammetry was performed from -1.0 to +1.0 V at 100 mV/s using PBS as background signal and on 1 mM hydrogen peroxide in PBS. The resulting voltammogram from this CV reveals that the curves for both hydrogen peroxide and background traces out the same profile across the potential range, with an exception of a reverse scan from 0 V to -1.0 V where the profiles diverge. A peak search function on NOVA 2.1, as well as a signal-to-background (S/B) ratio analysis reveals that the peak appears between -0.45 to -0.5 V in the cathodic (positive-to-negative) scan, with maximum S/B of 2.56. Potential of -0.45 V is then selected for hydrogen peroxide amperometric sensing.

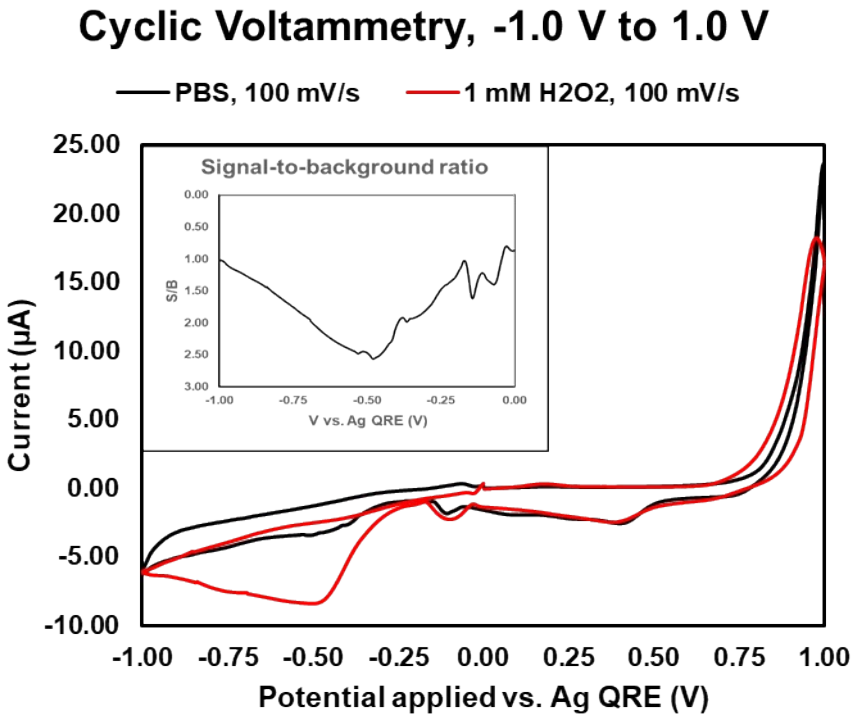

Figure S6. Cyclic voltammogram (n=1) of PBS and 1 mM hydrogen peroxide in PBS across a wide potential range. (Inset) The S/B ratio has a maximum of 2.56, at V = -0.479 V vs. Ag QRE.

Measuring inter-electrode gap size for circular electrodes

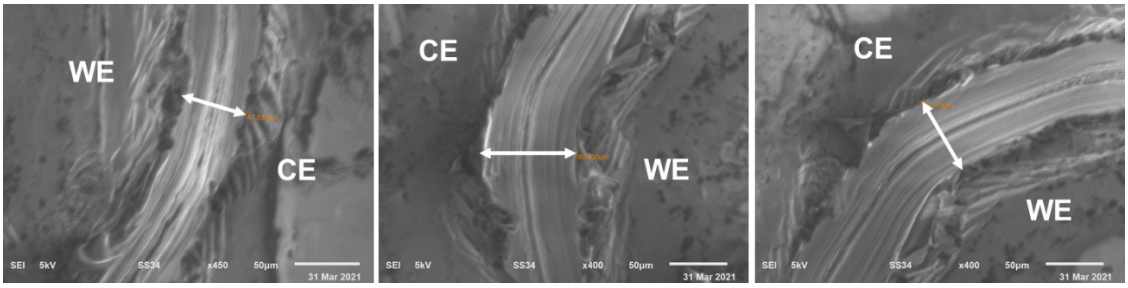

Figure S7. Scanning electron micrographs of inter-electrode gap between the circular working electrode and annulus counter electrode. White arrows indicate segment where the inter-electrode distance was measured. The gap sizes measured are 47.539 µm, 80.500 µm, and 66.115 µm respectively, resulting in a mean gap separation of 64.72 ± 13.49 µm. WE: working electrode, CE: counter electrode.

Determining gap size for Circuit Scribe electrodes

The size of minimum spacing between two adjacent Circuit Scribe silver electrodes that is electrically isolated from each other is experimentally determined (n = 2) by varying the CAD centre-to-centre distance between line electrodes and measuring the resistance across two adjacent electrodes with a multimeter. The minimum gap size is determined using CAD centre-to-centre distance instead of the width of the physical electrode to remove the variability in electrode/gap width due to the fabrication process. The minimum gap size is determined to be 800 µm in CAD distance.

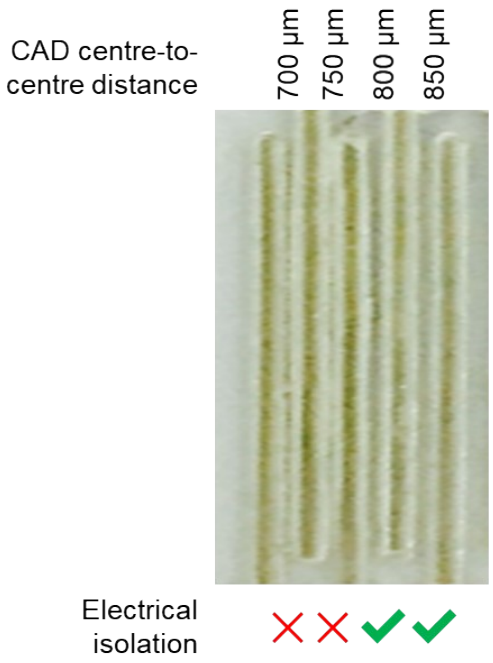

Figure S8. Minimum gap size determination of Circuit Scribe silver electrodes. The minimum spacing required for two adjacent electrodes to be electrically isolated is 800 µm in CAD centre-to-centre distance (n = 2).

Comparison of Limit of Detection and Sensitivity to Similar Works

Table S10. Comparison of limits of detection (LOD) and sensitivity of sensors against a selection of works in literature. For a fair comparison, for hydrogen peroxide sensors, only those that utilize enzyme-less gold electrode are compared. For glucose sensors, only those that uses a chitosan-embedded glucose oxidase enzymes on gold are included.

Analyte	Working electrode type	Limit of Detection	Sensitivity	Reference
Hydrogen peroxide	Electroplated nanoporous gold film	3.7 μM	400 μA mM^{-1} cm^{-2}	[8]
	Electroplated gold film	1 mM	1.37 nA mM^{-1}	[9]
	Gold leaf	713 μM	78.37 μA mM^{-1} cm^{-2}	This work
Glucose	Polished gold-chitosan-GOx	49.96 μM	8.91 μA mM^{-1} cm^{-2}	[10]
	Sputtered gold-tetrathiafulvalene-GOx	200 μM	n/a	[11]
	Porous gold-chitosan-MWCNT-Gox/HRP	25 μM	261.8 μA mM^{-1} cm^{-2}	[12]
	Gold leaf-chitosan-GOx	111 μM	12.68 μA mM^{-1} cm^{-2}	This work

MWCNT: multi-walled carbon nanotubes, GOx: glucose oxidase enzyme, HRP: horseradish peroxidase enzyme

References

1 A. K. Van der Vegt and L. E. Govaert, *Polymeren: van keten tot kunststof*, VSSD, Delft, 2005.
2 F. Awaja and D. Pavel, *European Polymer Journal*, 2005, **41**, 1453–1477.
3 E. L. V. Lewis, R. A. Duckett, I. M. Ward, J. P. A. Fairclough and A. J. Ryan, *Polymer*, 2003, **44**, 1631–1640.
4 A. J. Kinloch, *Adhesion and Adhesives*, Springer Netherlands, Dordrecht, 1987.
5 M. Akbari, D. Sinton and M. Bahrami, *Journal of Fluids Engineering*, 2009, **131**, 041202.
6 M.-B. Habhab, T. Ismail and J. F. Lo, *Sensors*, 2016, **16**, 1970.
7 C. A. Schneider, W. S. Rasband and K. W. Eliceiri, *Nat Methods*, 2012, **9**, 671–675.
8 A. Sukeri, A. S. Lima and M. Bertotti, *Microchemical Journal*, 2017, **133**, 149–154.
9 L. Rassaei and F. Marken, *Anal. Chem.*, 2010, **82**, 7063–7067.
10 Y. Zhang, Y. Li, W. Wu, Y. Jiang and B. Hu, *Biosensors and Bioelectronics*, 2014, **60**, 271–276.
11 E. Vargas, H. Teymourian, F. Tehrani, E. Eksin, E. Sánchez-Tirado, P. Warren, A. Erdem, E. Dassau and J. Wang, *Angew. Chem. Int. Ed.*, 2019, **58**, 6376–6379.
12 V. B. Juska and M. E. Pemble, *Analyst*, 2020, **145**, 402–414.